 Human Molecular Genetics, 2001, Vol. 10, No. 2 137–144

Neurological abnormalities in a knock-in mouse model of Huntington's disease

Chin-Hsing Lin[1], Sara Tallaksen-Greene[2], Wei-Ming Chien[1], Jamie A. Cearley[1], Walker S. Jackson[1], Andrew B. Crouse[1], Songrong Ren[1], Xiao-Jiang Li[3], Roger L. Albin[2,4] and Peter J. Detloff[1,5,+]

[1]Department of Biochemistry and Molecular Genetics and [5]Department of Neurobiology, University of Alabama at Birmingham, Birmingham, AL 35294, USA, [2]Department of Neurology, University of Michigan and [4]Geriatrics Research, Education and Clinical Center, Ann Arbor VAMC, Ann Arbor, MI 48104, USA and [3]Department of Genetics, Emory University, Atlanta, GA 30322, USA

Received 27 August 2000; Revised and Accepted 7 November 2000

Mice representing precise genetic replicas of Huntington's disease (HD) were made using gene targeting to replace the short CAG repeat of the mouse Huntington's disease gene homolog (*Hdh*) with CAG repeats within the length range found to cause HD in humans. Mice with alleles of ~150 units in length exhibit late-onset behavioral and neuroanatomic abnormalities consistent with HD. These symptoms include a motor task deficit, gait abnormalities, reactive gliosis and the formation of neuronal intranuclear inclusions predominating in the striatum. This model differs from previously described *Hdh* knock-ins by its method of construction, longer repeat length and more severe phenotype. To our knowledge, this is the first knock-in mouse model of HD to show increased glial fibrillary acidic protein immunoreactivity in the striatum, suggesting that these mice have neuronal injury similar to that found early in the course of HD. These mice will serve as useful reagents in experiments designed to reveal the molecular nature of neuronal dysfunction underlying HD.

INTRODUCTION

Huntington's disease (HD) is an autosomal dominant neurological disorder involving involuntary movements, psychiatric disturbances and cognitive impairment (1). Symptoms typically present during mid-life and progress to death 15–20 years after onset. Post-mortem analysis reveals degeneration in several areas of the brain, with prominent cell loss in the striatum (2). HD is caused by the inheritance of a CAG repeat between 36 and 180 units in length in exon 1 of a gene of unknown function called huntingtin (3,4). Longer repeats are associated with earlier ages at onset (3). The repeat codes for a polyglutamine stretch near the N-terminus of the huntingtin protein, which contributes to protein aggregates found in affected regions of patient brains (5,6). Evidence indicates that the HD mutation acts by a toxic gain of function, rather than by a loss of HD gene function (7). The molecular steps mediating neurotoxicity remain unknown.

Clues as to the molecular mechanism underlying HD have come from the analysis of mouse lines engineered to express additional copies of partial or full-length versions of mutant huntingtin (8). Determining the molecular cause of neuronal dysfunction in transgenic mouse models requires caution, however, since transgenic mice can have complicating phenotypes. For example, in some strain backgrounds an HD transgene with long repeats can cause diabetes (9). In this case the molecular consequences of insulin loss must be taken into account when analyzing this line. Inappropriate expression of any HD transgene might cause other, as yet unrevealed, abnormalities by molecular mechanisms that differ from those in HD. In the transgenic mouse models of HD described to date, abnormalities are seen only when expression levels of mutant HD transgenes approximate or exceed the expression of the endogenous mouse HD homolog (*Hdh*) (8). Each of these lines can be considered to be overexpressors of huntingtin, since the transgene is expressed in addition to the mouse *Hdh* locus. This differs from HD in man, which does not involve such increases in expression (10). The additional expression in transgenic mice might potentiate a polyglutamine toxicity by a mechanism not representative of the molecular processes underlying HD.

Given the powerful impetus of the lack of knowledge of the molecular causes of neuronal dysfunction in transgenic mouse models of HD, several groups have taken the strategy of making the best possible genetic replica of the disease. Gene targeting has been used to insert pathogenic sized CAG repeats into the *Hdh* locus (11–13), resulting in 'knock-in' mice. One group has shown nuclear localization of the normally cytoplasmic huntingtin protein and late-onset nuclear inclusion formation in the striatal neurons of mice with repeats from 90 to 111 units in length. These molecular changes occurred in the absence of overt behavioral abnormalities (11). Another group has reported non-ubiquitinated Hdh protein deposited as neuronal intranuclear inclusions (NIIs) and neuropil aggregates (14). Mild functional changes in the neurons of Hdh knock-in mice have been reported (13,15). The usefulness of these models in testing drug efficacy is limited by the highly focused

[+]To whom correspondence should be addressed. Tel: +1 205 975 8157; Fax: +1 205 975 7928; Email: pdetloff@bmg.bhs.uab.edu

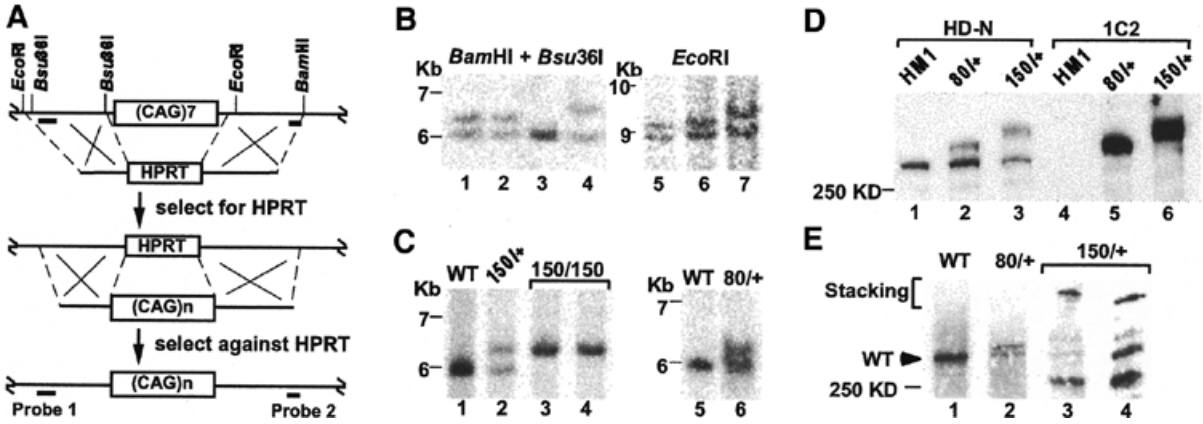

Figure 1. Gene targeting and expression of *Hdh* mutant alleles. (**A**) Diagram of the double replacement gene targeting strategy. Lines showing break marks on their ends represent the *Hdh* exon 1 region in an ES cell chromosome. Lines without break marks indicate gene targeting constructs. X indicates a crossover point. The homology driving the gene targeting reaction is delimited by dashed lines. Boxes indicate the *Hdh* exon 1 with a short repeat [(CAG)7], the Hprt minigene (HPRT) (16) and *Hdh* exon 1 with long repeats [(CAG)n]. (**B**) Southern analysis of ES cell clones used to produce mouse lines. Bands in lanes 1–4 represent ES cell DNA digested with *Bam*HI and *Bsu*36I and hybridized to probe 2. Bands in lanes 5–7 represent ES cell DNA digested with *Eco*RI and hybridized to probe 1. The targeted ES cell lines eCL1 (lanes 1 and 5) and eCL8 (lanes 2 and 6) are heterozygous for the $Hdh^{(CAG)80}$ allele. The targeted ES cell line eCL2 (lanes 4 and 7) is heterozygous for the $Hdh^{(CAG)150}$ allele. Lane 3 represents DNA from the starting ES cell line HM1 (16). (**C**) Genotyping mouse tail DNA by Southern analysis. Probe 2 was used to detect *Bam*HI–*Bsu*36I fragments containing *Hdh* exon 1 from wild-type mice (lanes 1 and 5), heterozygous (lane 2) and homozygous (lanes 3 and 4) CHL2 mutants and heterozygous CHL1 mice (lane 6). (**D**) Western analysis of ES cell protein. Protein from the wild-type HM1 ES cell line (lanes 1 and 4), the eCL1 cell line (lanes 2 and 5) and the eCL2 cell line (lanes 3 and 6) probed with the HD-N antibody (lanes 1–3) or the 1C2 antibody (28) (lanes 4–6). (**E**) Western analysis of brain protein. The N-terminus of Hdh protein was detected with the HD-N antibody from whole brain extracts of a wild-type (lane 1), a CHL1 heterozygote (lane 2) and CHL2 heterozygotes aged 34 weeks (lane 3) and 45 weeks (lane 4). The bracket represents the stacking gel and the arrow indicates the 350 kDa wild-type Hdh protein.

nature of the assays used to reveal their abnormalities. For example, a treatment that inhibited nuclear inclusion formation might have little or no effect in treating HD. Furthermore, these assays require the sacrifice of mice in order to measure the effect of potential treatments. This reliance on *ex-vivo* assays precludes the validation of a treatment by the elimination of symptoms of a live mouse. To date the only report of an abnormality in a live *Hdh* knock-in line has been increased male aggression (12). This finding contradicts the results of Wheeler *et al.* (11), who studied an *Hdh* knock-in line with a similar sized repeat and found no detectable behavioral abnormalities in studies that included a test for male aggression. Together, the phenotypes of the *Hdh* knock-in mice reported to date suggest a pre-symptomatic state.

This work describes the production and analysis of a knock-in model of HD with abnormalities measurable in a live mouse and neuropathological features consistent with HD in man. The strategy used to make these mice included replacement of the short repeat of the *Hdh* gene with a repeat of greater length than previously described in *Hdh* knock-in models. Our line with a 150 unit CAG repeat exhibits several abnormalities, including a motor task deficit, gait abnormalities, activity disturbances, reactive gliosis and the formation of NIIs predominantly in the striatum. Consistent with the presentation of HD symptoms in man, the abnormalities in this mouse model are late onset and repeat length dependent.

RESULTS AND DISCUSSION

Knock-in and expression of long CAG repeat alleles

The short CAG repeat in exon 1 of the mouse *Hdh* locus was replaced with long CAG repeats using a two-step gene targeting strategy (16). In the first step of this protocol we used standard gene targeting to replace exon 1 of the *Hdh* locus with the selectable marker Hprt. Embryonic stem (ES) cells with this modification were then used in the second round of gene targeting, resulting in the replacement of the Hprt marker with the long repeat versions of *Hdh* exon 1 (Fig. 1A). The use of this gene targeting strategy resulted in ES cells with alleles that differed from the wild-type *Hdh* locus only in the size of the CAG repeat (Fig. 1B). ES cell lines carrying the $Hdh^{(CAG)80}$ allele were used to make the mouse line CHL1, and an ES cell line carrying the $Hdh^{(CAG)150}$ allele was used to make the mouse line CHL2 (Fig. 1C).

Expression of mutant Hdh protein was confirmed by western analysis in both ES cells and the brains of mutant mice. In ES cells, Hdh protein was detected with the antibody HD-N, which recognizes the N-terminus of Hdh protein and, separately, with the anti-polyglutamine antibody 1C2 (Fig. 1D). This analysis confirmed that the inserted CAG repeats were expressed as a polyglutamine tract in the full-length Hdh protein. Western analysis of brain protein using the HD-N antibody confirms the expression of the mutant allele at levels similar to those of the wild-type protein (Fig. 1E). The lanes representing the CHL2 heterozygotes show immunoreactivity in the stacking gel not revealed in lanes representing CHL1 or wild-type brains. This immunoreactive band may represent Hdh protein aggregates too large to enter the separating gel, a phenomenon previously reported for HD protein from patient material (5).

Neurological assessment

A set of three tests was performed on mice of varying age and genotype once a day for a total of 10 days. The first test measured activity of mice just after removal of the cage lid. In this situation,

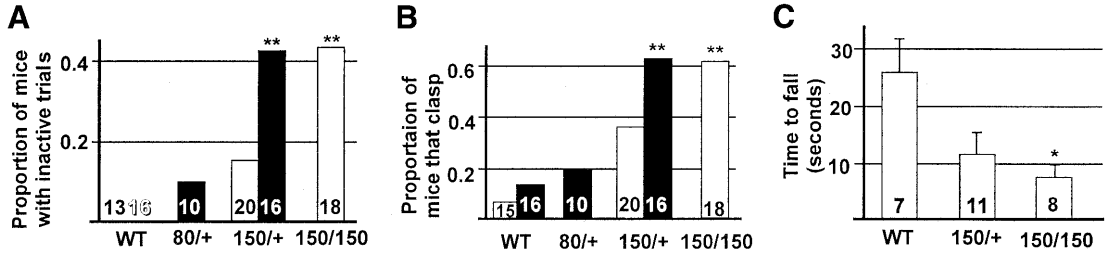

Figure 2. Behavioral characteristics of *Hdh* mutants. (**A**) The proportion of mice tending to remain inactive on opening the cage. (**B**) The proportion of mice tending to clasp during tail suspension. (**C**) The mean time to fall from the 5.0 r.p.m. rotating rod. Error bars indicate the standard error of the mean (SEM). The number of mice is shown at the base of the bar. Filled bars indicate mice older than 40 weeks, and open bars indicate mice between 15 and 40 weeks of age. Significant differences compared with wild-type mice of the same age are indicated above the bars (*$P < 0.05$; **$P < 0.01$; Kruskal–Wallis non-parametric ANOVA with Dunn's multiple comparison test).

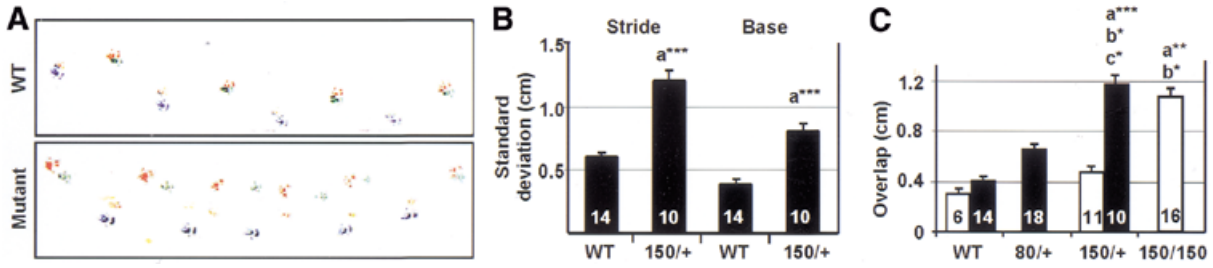

Figure 3. Gait abnormalities in *Hdh* mutants. (**A**) Paw placement records of a 1-year-old wild-type (top) and an age-matched affected CHL2 heterozygote (bottom). Each color represents a different paw (orange, right front; green, left front; blue, right hind; red, left hind). (**B**) Variation of stride and base lengths. (**C**) Mean distance between placement of front and hind paw. Filled bars indicate mice older than 40 weeks and open bars indicate mice between 15 and 40 weeks of age. Significant differences by Kruskal–Wallis non-parametric ANOVA with Dunn's multiple comparison test are shown by asterisks above the bars (*$P < 0.05$; **$P < 0.01$; ***$P < 0.001$; a, comparison with wild-type of same age; b, comparison with young $Hdh^{(CAG)150}$ heterozygotes; c, comparison with old $Hdh^{(CAG)80}$ heterozygotes). Error bars indicate SEM and the number of mice is indicated at base of each bar.

normal mice exhibit exploratory activity involving walking around their cage (17). As shown in Figure 2A, wild-type mice were always active, and only 1 of 10 heterozygous CHL1 mice had an inactive trial. A few young (15–40 weeks of age) heterozygous CHL2 mice had inactive trials, and the proportion of inactive mice increased to a level that significantly differed from that of wild-type mice when CHL2 heterozygotes were old (>40 weeks of age). These results indicate that the tendency to be inactive in the context of this test is a late-onset trait conferred by the $Hdh^{(CAG)150}$ mutant allele. CHL2 homozygotes show this tendency to be inactive prior to 40 weeks of age, suggesting that an increase in mutant allele dose causes an earlier onset of this abnormality.

The second test involved the response of the mouse to a 1 min tail suspension. During tail suspension, normal mice will struggle, with flailing limb movements. Mice with neurological problems will sometimes maintain a position with paws pressed against the body, termed 'clasping'. As shown in Figure 2B, <20% of wild-type or CHL1 mice tend to clasp. This contrasts with >60% of the old heterozygous and young homozygous CHL2 mice. These results show that the $Hdh^{(CAG)150}$ allele causes a late-onset tendency to clasp and that CHL2 homozygotes have an earlier onset than heterozygotes.

The third test involved measuring the amount of time a mouse could stay on a slowly rotating rod (17). At 2.5 r.p.m., old wild-type mice averaged 40 s on the rod and old heterozygous CHL2 mice averaged 32 s. Due to the great variability from mouse to mouse, however, this difference did not reach statistical significance. A second trial with a more limited number of CHL2 mice was performed with a speed of 5.0 r.p.m. The graded decrease in time on the rod with the increasing mutant gene dosage (Fig. 2C) shows that the $Hdh^{(CAG)150}$ mutation causes deficits in performance of this motor task.

One of the most obvious symptoms of HD is an abnormal gait (1). Gait disturbances were measured by making a permanent record of paw placement during walking. The paws of a subject were painted prior to having it walk in a paper-lined corridor. The normal gait representative of all wild-type mice in this study is shown in Figure 3A (top) compared with prints of an old CHL2 heterozygote with an abnormal gait (Fig. 3A, bottom). Measurements of stride length, base length and the distance between front and hind paw placement (overlap length) were made. The mean stride and base lengths did not differ for mutant and wild-type mice. As a measure of variability, the standard deviations of stride and base length were calculated for each mouse. Standard deviations of stride and base lengths for old CHL2 heterozygotes were about twice those of old wild-type controls (Fig. 3B). Young mice show no differences in stride and base length variation, suggesting that the $Hdh^{(CAG)150}$ mutation causes a late-onset variability in gait. A late-onset increase was also seen in the average distance between front and hind paws, a measure we refer to as

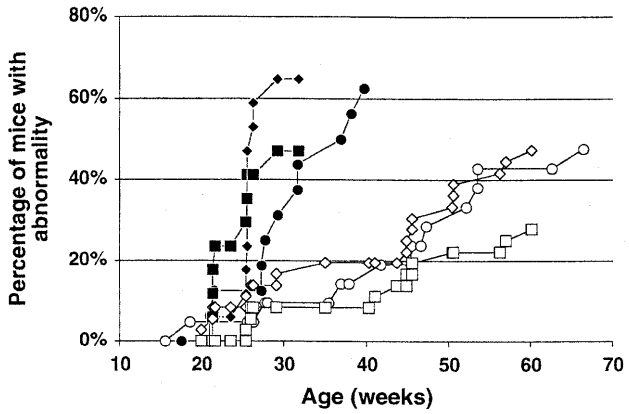

Figure 4. Onset of abnormalities in the CHL2 line. Percentage of assayed mice that exhibit the abnormality by the specified age. Filled symbols indicate $Hdh^{(CAG)150}$ homozygotes and open symbols indicate $Hdh^{(CAG)150}$ heterozygotes. Diamonds represent mice in a tail suspension trial. Mice were classified as abnormal if they clasped in one or more of ten trials (18 homozygotes, 35 heterozygotes). Circles represent mice in the gait analysis trials (16 homozygotes, 21 heterozygotes). A gait overlap mean of >0.8 cm was considered abnormal. Squares represent mice in the open cage activity trial (18 homozygotes, 35 heterozygotes). Mice that were inactive in one or more of the ten trials were considered abnormal.

'overlap' (Fig. 3C). The increase in overlap distance is dependent on repeat length, as shown by the significant difference between the old CHL1 and CHL2 heterozygotes (Fig. 3C). This abnormality affects CHL2 homozygotes at an earlier age than heterozygotes, suggesting an acceleration of onset caused by the additional dose of the $Hdh^{(CAG)150}$ allele (Fig. 3C).

This assessment of the population of mutant animals shows that the $Hdh^{(CAG)150}$ mutation causes several neurological abnormalities. The age of presentation of symptoms in the CHL2 line is shown in Figure 4. These data suggest a median age at onset of 60 weeks for heterozygotes and 25 weeks for homozygotes. Individual mutant mice can show some or all of these abnormalities, suggesting variation in presentation of symptoms. This variation may reflect a difference in age of presentation for an individual trait or some other unknown genetic or environmental factor. The presence of gait abnormalities is a good predictor of the other measured abnormalities. Nine of the ten CHL2 mice with the most severe gait disturbance (as measured by overlap of front and hind paws) showed either clasping or open cage inactivity. Therefore, the described abnormalities make up part of a cumulatively predictable set of symptoms in these mice.

The nature of the CHL2 abnormalities differentiate this model from previous knock-in mouse models of HD. To date, the only reported behavioral abnormality in a knock-in mouse model of HD is increased male aggression (12). One could think of many treatments (e.g. a mild sedative) that would eliminate this symptom without affecting the underlying cause. In contrast, the CHL2 mice have several abnormalities, including motor task deficits and gait disturbances, that would most likely be remedied only by a re-establishment of proper neuronal function.

Homozygotes

Previous work has shown that large reductions in expression of the *Hdh* locus cause severe problems with neuronal development (18). If long repeats cause a similar inactivation of the locus, we might expect CHL2 homozygotes to exhibit similar problems with neuronal development. Matings of CHL2 heterozygotes yielded 23 wild-type, 54 heterozygous and 21 homozygous mutant offspring. Since these numbers are roughly the expected 1:2:1 Mendelian ratio, the $Hdh^{(CAG)150}$ mutant allele causes no large reduction in viability when homozygous. All of the CHL2 homozygotes appeared to develop normally, showing that CAG repeats up to 150 units in length do not significantly impair *Hdh* function. This result extends the observation of White *et al.* (18), who showed that a repeat of 50 CAGs did not impair *Hdh* function. Unlike the 50 unit CAG repeat length, which causes no observable phenotype in mice, the 150 unit length repeat allele causes the late-onset abnormalities described above. Together, these results suggest that the late-onset abnormalities in the CHL2 line are due to a toxic gain of function rather than a partial loss of *Hdh* function.

Each of the four abnormalities described above showed an earlier onset in $Hdh^{(CAG)150}$ homozygotes than in heterozygotes. An acceleration of onset has also been reported with increased expression from HD transgenes (8). In contrast, humans homozygous for the HD mutation have been reported to have similar ages at onset to those of heterozygotes (19). This discrepancy might be due to an inherent difference between mouse and man or an accelerated onset might occur only when repeats of very long length are increased in dose. It is also possible that there is an accelerated phenotype in human homozygotes, obscured by the great variability in age at onset for a given repeat size in heterozygous individuals (3).

General observations

A substantial proportion of juvenile-onset HD victims have seizures (1). Infrequently, during handling, a mouse would have a convulsive spell consistent with a tonic–clonic seizure. A rough quantitative estimate of convulsive spell frequency is provided by the rotating rod trials. Spells occurred in 4 of 25 $Hdh^{(CAG)150}$ mice assayed (250 trials), in 1 of 10 $Hdh^{(CAG)80}$ mice (100 trials) but were never observed in the 23 wild-type mice assayed (230 trials). These occurred in mice aged from 25 to 60 weeks and two $Hdh^{(CAG)150}$ mutants had more than one occurrence during their 10 trials. These data suggest that the inserted repeats cause seizure susceptibility.

HD victims tend to lose weight with the progression of the illness (20). We found that the $Hdh^{(CAG)150}$ mutation was associated with mice of slightly lower weight (Fig. 5). This difference in weight is most likely due to a few mutant mice showing large reductions in weight. After 25 weeks of age, ~1 in 10 mutants was noticeably smaller than its wild-type littermate(s), and this difference increased slowly over a period of weeks. Some CHL1 and CHL2 mutants, but no wild-type mice, showed obvious size reductions, suggesting that this is a low penetrance trait associated with both the 80 and 150 unit CAG repeat mutations.

Previous studies of a transgenic HD mouse model showed that the mice suffered from insulin-dependent diabetes (9). To determine whether the mice in CHL1 and CHL2 colonies also had diabetes, we monitored the random blood glucose levels of

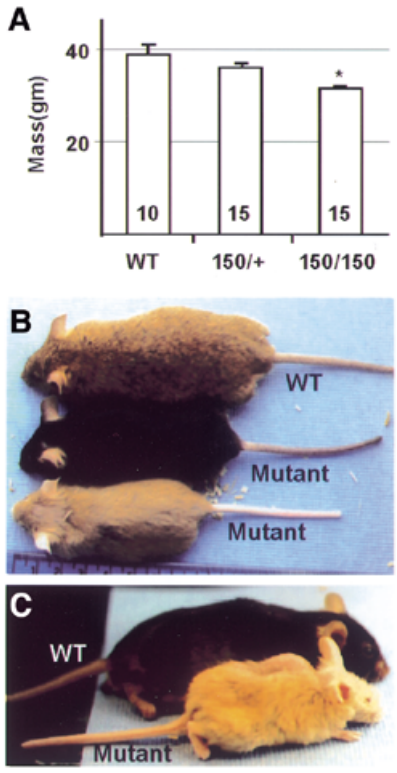

Figure 5. Mass and size decrease for *Hdh* mutants. (**A**) Mass of males at 25–30 weeks of age. Error bars indicate SEM and the number of mice is indicated at base of each bar. Significant differences compared with wild-type mice of the same age are shown by an asterisk above the bar ($P = 0.035$; Kruskal–Wallis non-parametric ANOVA with Dunn's multiple comparison test). (**B**) Wild-type mouse and $Hdh^{(CAG)150}$ heterozygous littermates exhibiting noticeable size differences at 52 weeks of age. (**C**) Wild-type mouse and $Hdh^{(CAG)80}$ heterozygous littermates exhibiting extreme size difference at 34 weeks of age.

24 mice of varying age, weight and genotype. The blood glucose levels of CHL1 and CHL2 mutants were normal.

HD causes premature death in humans (3). The mice in the CHL2 colony are not yet old enough for a determination of their age at death. Only 3 of 45 CHL2 heterozygotes died prior to 1 year of age, showing that the typical lifespan of this line is >1 year. Homozygotes of this line are now much younger than the heterozygotes and it is possible, given their accelerated age at onset, that they will show an earlier age at death than heterozygotes.

Neuroanatomical analysis

HD causes neuron loss in several brain regions, but the most vulnerable are the medium sized neurons of the striatum. Loss of these cells is typically so extreme as to cause a visible decrease in striatal volume and a corresponding increase in the volume of the lateral ventricles (2). Extreme reductions in major brain regions were not observed in CHL1 heterozygotes up to 90 weeks of age, nor in CHL2 mice up to 52 weeks of age. Furthermore, cell counts suggest no loss of neurons. Determination of the actual density and number of neurons, however, requires application of unbiased stereology methods. We are pursuing extensive anatomic characterization of striatal changes in these animals, and determination of the actual extent of neuronal survival (or loss) awaits the results of this analysis. Since some HD victims show only subtle evidence of neurodegeneration (2), mice were analyzed for reactive gliosis, one of the early markers of central nervous system damage in HD (21). Immunocytochemistry to detect glial fibrillary acidic protein (GFAP) was performed on 5 CHL1, 10 CHL2 mutants and 5 wild-type controls. There was a marked increase in GFAP immunoreactivity in the striatum of CHL2 mutants compared with CHL1 and wild-type controls (Fig. 6). Most CHL2 mutants showed restricted areas of intense staining in the striatum (Fig. 6B). This staining is reminiscent of patches of GFAP staining seen in the brains of HD victims (21). An example of a CHL2 mutant with intense staining throughout the striatum is shown in Fig. 6C. The presence of gliosis and relative preservation of neuronal number is analogous to early-onset HD.

A common feature of all polyglutamine repeat disorders is the presence of aggregates of the polyglutamine-containing portion of the disease protein (22). Two types of this aggregate, NIIs and dystrophic neurites (DNs), have been found in post-mortem HD (5,6). Both structures contain ubiquitin and are typically found in areas of the brain vulnerable to degeneration, including the striatum (5). Aggregates have also been found in transgenic mice expressing long repeat versions of the huntingtin gene (8,23). It is not clear what role NIIs play in the pathological processes of HD. Proposals range from a direct toxic intermediate, to a point of sequestration of a toxic product, thereby being beneficial to a neuron (17,24). The most striking neuroanatomical phenotype observed in our *Hdh* knock-in model is the presence of ubiquitin- and huntingtin-positive nuclear inclusions throughout the dorsal striatum and nucleus accumbens (Fig. 7). NIIs were less frequent in other brain regions of the old CHL2 mutants, such as the neocortex, where inclusions were restricted to neurons in layers III and IV of the somatosensory cortex. In the allocortex, NIIs were abundant in the rostral part of the piriform cortex. Fewer inclusions were seen in the subiculum and in the pyramidal cell layer of the hippocampus. In the cerebellum, NIIs were present in neurons of the deep nuclei and in the granular cell layer of the cortex. Inclusions were generally sparse in the thalamus, hypothalamus and brainstem. No evidence was found for DNs in these brains. The predominance of NIIs over DNs in these animals is reminiscent of juvenile HD victims (5). NIIs were rarely observed in $Hdh^{(CAG)80}$ mutants up to 90 weeks of age and no NIIs were observed in wild-type controls, showing that NII formation is repeat length dependent. NIIs were also not observed in CHL2 mutants younger than 40 weeks of age. Similar to the behavioral abnormalities described above, NII formation in these mice is dependent on age, with an onset at ~40 weeks.

NIIs represent products of a mislocalized portion of the normally cytoplasmic huntingtin protein (22). A critical role for this mislocalization is suggested by several reports of reductions in toxicity by the prevention of nuclear accumulation of proteins containing polyglutamine (8). In a previous study, the anti-huntingtin antibody EM48 revealed diffuse nuclear staining in a knock-in mouse model of HD (11). Using the same antibody, we observed a similar pattern of staining in the striatum of CHL2 mice that is not present in wild-type controls (Fig. 7). Diffuse nuclear huntingtin immunoreactivity was

consistently found in neurons with NIIs in the older CHL2 mice and also in neurons of young CHL2 mice which lack NIIs. Furthermore, the striatal nuclei of young CHL2 mice did not stain with the anti-ubiquitin antibody. Together these results show that a non-ubiquitinated form of the mutant Hdh protein is present in the nucleus prior to aggregation. This mislocalized protein might be processed into NIIs as the disease progresses.

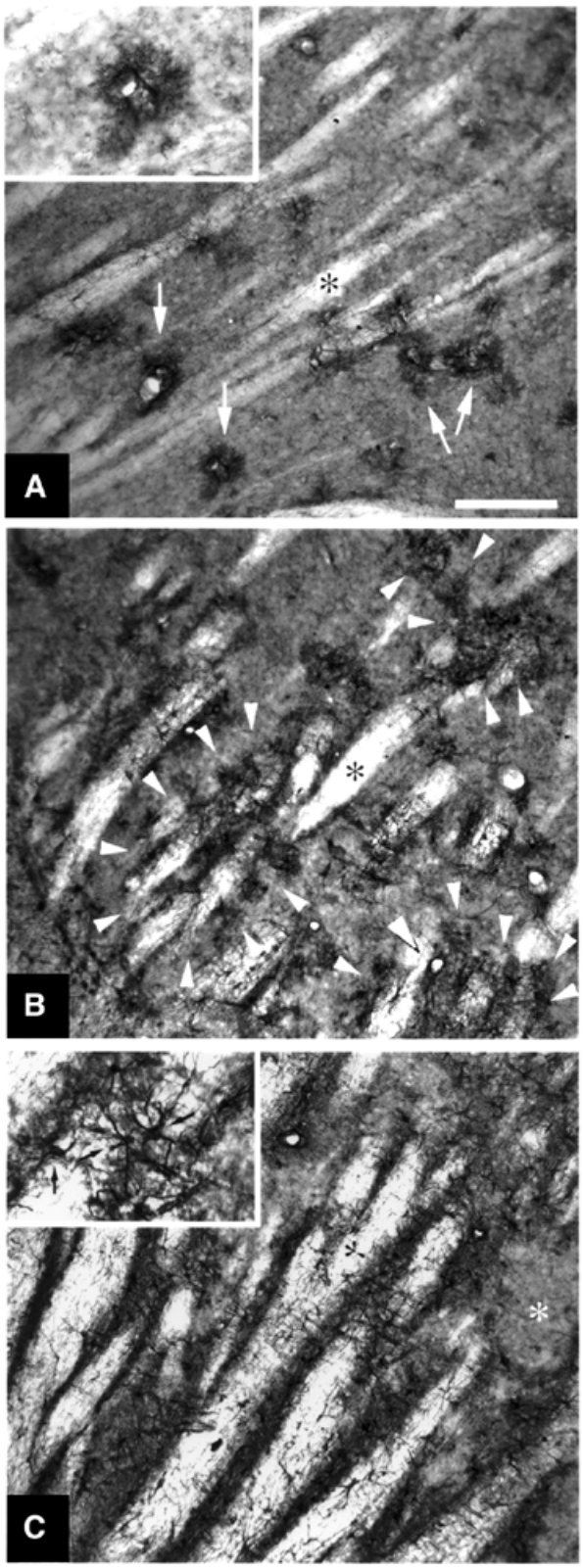

Concluding remarks

The phenotype of the CHL2 line is less severe and presents later than that of mice, with 150 unit repeats expressed from either the *Hprt* locus (17) or a transgene consisting of exon 1 of the *HD* locus (25). The differences in severity of phenotype might be a direct consequence of differences in levels of expression. This explanation seems unlikely given that the levels of expression of the *HD* exon 1 transgene were comparable to endogenous Hdh levels (25). The more severely affected transgenic models share the common feature of having the polyglutamine expressed in the context of a small protein. Thus, it is possible that the large size of the full-length Hdh protein acts to diminish a polyglutamine toxicity, as proposed for the Machado–Joseph disease protein (26). The phenotype described here for the $Hdh^{(CAG)150}$ mouse is more severe than that described for Hdh knock-ins with shorter repeats, suggesting that further increases in repeat length might be used to produce mice with earlier ages at onset. The CHL2 line will be a valuable reagent in helping to determine the as yet unknown molecular mechanisms underlying neural dysfunction in HD. Furthermore, the late-onset neurological abnormalities displayed by these mice provide both end-stage neuroanatomical features and a set of simple non-invasive behavioral assays that will be valuable in the assessment of therapies designed to cure HD.

MATERIALS AND METHODS

Construction of mutant mice

Gene targeting constructs with varying lengths of repeat were produced and confirmed by sequencing. PCR-based mutagenesis was used to replace the entire CAG repeat of *Hdh* with the sequence 5′-CAGGATCCAGCAG-3′. Digestion with *Bam*HI and S1 nucleases allowed insertion of long CAG repeats (27) to the added sequence by blunt-end ligation. The resulting targeting constructs contained 5.6 kb of homology upstream of the repeat and 5.5 kb of homology downstream of the repeat. Mutations were introduced to the *Hdh* locus by a two-step gene targeting strategy (16). First, conventional gene targeting was used to replace the 1.4 kb *Kpn*I–*Pst*I fragment containing exon 1 of the murine *Hdh* gene with an Hprt minigene in the *Hprt*-deficient ES cell line HM1 (gifts from D.W. Melton). Second, gene targeting using long repeat variants of exon 1 were used to replace the Hprt minigene in an ES cell line targeted during

Figure 6. GFAP immunostaining is increased in striatum of CHL2 mutants. (**A**) In wild-type controls, GFAP astrocytes (white arrows) are most frequently observed in association with blood vessels (inset) or along fiber bundles (black asterisk). (**B**) Islands of dark GFAP immunoreactivity (white arrowheads) are commonly seen throughout the striatum of mutant mice. The islands vary in size and staining intensity but are most often observed in association with white matter fiber bundles. (**C**) An example of a more severely affected region of stratum in a CHL2 mouse. GFAP staining is heavy throughout the neuropil except in isolated patches (white asterisk). Clumps of darkly stained astrocytes (inset) are visible. Bar: 275 μm (A–C), 125 μm (insets).

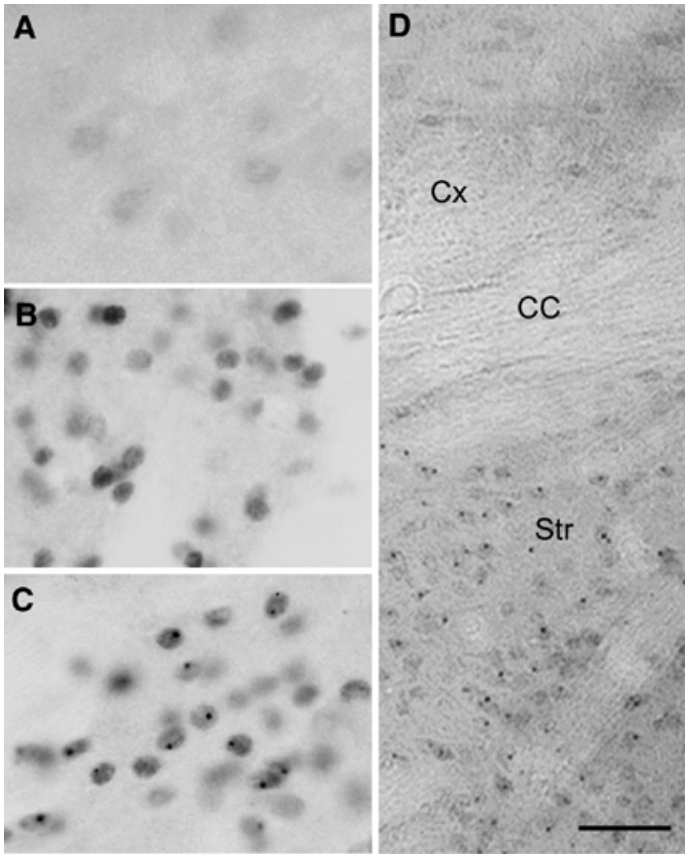

Figure 7. Nuclear inclusions in *Hdh* mutant brains. (A–C) Striatum stained with anti-huntingtin antibody EM48. (**A**) 51-week-old wild-type. (**B**) Diffuse nuclear staining in a 31-week-old CHL2 heterozygote. (**C**) NIIs in stained nuclei of a 51-week-old CHL2 heterozygote. (**D**) Striatal specificity of nuclear inclusions in a 51-week-old CHL2 heterozygote stained with anti-ubiquitin antibody. Cx, cerebral cortex, CC, corpus callosum, Str, striatum. Bar: 25 μm (A–C), 50 μm (D).

the first round. Targeted ES cells were confirmed by Southern blot analysis and injected into C57BL/6J blastocysts, which were transferred to the uteri of pseudopregnant females to complete development. Resulting chimeras were mated to C57BL/6J mice, making carriers of long repeat mutations a combination of 129/Ola from HM1 ES cells and C57BL/6J.

Western analysis

Proteins obtained from ES cells or whole mouse brain were separated on a 4–8% gradient SDS–polyacrylamide gel, subsequently transferred to nitrocellulose paper and probed with the antibodies HD-N (using a 1:1000 dilution) or 1C2 (using a 1:2000 dilution). The HD-N antibody was made by immunization of rabbits with a peptide consisting of the first 17 amino acids of the Hdh protein followed by affinity purification using this same peptide (Research Genetics), and the anti-polyglutamine antibody 1C2 (28) was purchased from Chemicon. Autoradiography and the Enhanced Chemiluminescence kit from Amersham was used for western blot detection.

Behavioral analysis

Mice of varying age and genotype were assayed once per day for 10 consecutive days. The young mice aged 25–40 weeks included 20 CHL2 heterozygotes, 18 CHL2 homozygotes and 15 wild-types. Mice aged 40–65 weeks included 16 CHL2 heterozygotes, 10 CHL1 heterozygotes and 16 wild-types. Each mouse was housed in a closed cage, which would be opened in a well-lit laminar flow hood. Mice were scored as inactive if they did not walk from their original position during the first 30 s in one or more of the ten trials. Each mouse was suspended by the tail and was classified as tending to clasp if, during any one of its ten trials, the mouse stopped struggling and held its front paws together near its torso. Usually once a mutant mouse clasped it would continue for the duration of the trial. Mice were placed on a slowly rotating (5 r.p.m.) rod 4.0 cm in diameter and time to fall was recorded. If a mouse stayed on the rod at the end of the 1 min trial, then a time of 60 s was recorded. Since wild-type mice improve in performance during the initial trials (17), the first three trials were excluded as training trials.

For the analysis of gait, paws of a subject were painted prior to placing it in a paper-lined runway (length 96 cm, width 10 cm, height 10 cm). Mice would walk towards the open end of the corridor leaving a permanent record of their paw placement. To obtain statistically useful information, measurements between pawprints were made on seven legible strides. Stride length is the distance between adjacent prints made by the same paw. Base length includes measurement within each stride of front paw to opposite front paw distance and separately hind paw to hind paw distance. Overlap is a measure of the distance between the front and hind paw.

Blood glucose measurements

Tail vein blood was analyzed with a hand-held blood glucose monitor (One Touch; Johnson & Johnson) according to the manufacturer's instructions. Random blood glucose levels for mice between 27 and 56 weeks of age were 94 ± 12 mg/dl for CHL1 heterozygotes (n = 6), 83 ± 10 mg/dl for CHL2 heterozygotes (n = 7) and 90 ± 13 mg/dl for wild-types (n = 11).

Neuroanatomic analysis

The brains of three young (27–30 weeks) and three old (42–52 weeks) CHL2 heterozygotes, three old (42–52 weeks) and four very old (80–91 weeks) wild-type controls and eight very old (80–90 weeks) CHL1 heterozygotes were anesthetized, then fixed with 4% paraformaldehyde by transcardial perfusion and subsequently cryoprotected in 20% sucrose. Sections of 30–40 µM were cut in the horizontal plane. Staining with the anti-HD antibody EM-48 (1:100) (23), an anti-ubiquitin antibody (1:1000; Dako) and an anti-GFAP antibody (10 µg/ml; Calbiochem) was visualized by diaminobenzidine staining using a peroxidase-conjugated secondary antibody and the IgG Elite ABC kit (Vector Laboratories).

ACKNOWLEDGEMENTS

This work is dedicated to the memory of John B. Penny. We would like to thank Drs Jared Ordway, Gail Johnson, Mathieu Lesort, JinXiang Ren and Kevin Pawlik for technical assistance, Dr Tim Townes for use of the microinjection equipment and Dr David Melton for the gift of the Hprt minigene and the HM1 ES cell line. This work was supported by grants from the Hereditary Disease Foundation, the Wills Foundation, the Huntington's Disease Society of America, the Hereditary Disease Foundation Cure HD initiative and NIH/NINDS grants R01 NS34492 (P.J.D.) and RO1 NS38166 (R.L.A.).

REFERENCES

1. Quarrell, O. and Harper, P. (1991) The clinical neurology of Huntington's disease. In Harper, P.S. (ed.), *Huntington's Disease*. W.B. Saunders, London, Vol. 22, pp. 37–80.
2. Quarrell, O. (1991) The neurobiology of Huntington's disease. In Harper, P.S. (ed.), *Huntington's Disease*. W.B. Saunders, London, Vol. 22, pp. 141–178.
3. Gusella, J.F., McNeil, S., Persichetti, F., Srinidhi, J., Nevelletto, A., Bird, E., Faber, P., Vansattel, J.-P., Myers, R.H. and MacDonald, M.E. (1996) Huntington's disease. *Cold Spring Harb. Symp.*, **61**, 615–626.
4. Sathasivam, K., Amaechi, I., Mangiarini, L. and Bates, G. (1997) Identification of an HD patient with a $(CAG)_{180}$ repeat expansion and the propagation of highly expanded CAG repeats in lambda phage. *Hum. Genet.*, **99**, 692–695.
5. DiFiglia, M., Sapp, E., Chase, K.O., Davies, S.W., Bates, G.P., Vonsattel, J.P. and Aronin, N. (1997) Aggregation of huntingtin in neuronal intranuclear inclusions and dystrophic neurites in brain. *Science*, **277**, 1990–1993.
6. Maat-Schieman, M.L., Dorsman, J.C., Smoor, M.A., Siesling, S., Van Duinen, S.G., Verschuuren, J.J., den Dunnen, J.T., Van Ommen, G.J. and Roos, R.A. (1999) Distribution of inclusions in neuronal nuclei and dystrophic neurites in Huntington disease brain. *J. Neuropathol. Exp. Neurol.*, **58**, 129–137.
7. Ambrose, C.M., Duyao, M.P., Barnes, G., Bates, G.P., Lin, C.S., Srinidhi, J., Baxendale, S., Hummerich, H., Lehrach, H., Altherr, M. *et al.* (1994) Structure and expression of the Huntington's disease gene: evidence against simple inactivation due to an expanded CAG repeat. *Somat. Cell Mol. Genet.* **20**, 27–38.
8. Lin, X., Cummings, C.J. and Zoghbi, H.Y. (1999) Expanding our understanding of polyglutamine diseases through mouse models. *Neuron*, **24**, 499–502.
9. Hurlbert, M.S., Zhou, W., Wasmeier, C., Kaddis, F.G., Hutton, J.C. and Freed, C.R. (1999) Mice transgenic for an expanded CAG repeat in the Huntington's disease gene develop diabetes. *Diabetes*, **48**, 649–651.
10. Landwehrmeyer, G.B., McNeil, S.M., Dure, L.S., Ge, P., Aizawa, H., Huang, Q., Ambrose, C.M., Duyao, M.P., Bird, E.D., Bonilla, E. *et al.* (1995) Huntington's disease gene: regional and cellular expression in brain of normal and affected individuals. *Ann. Neurol.*, **37**, 218–230.
11. Wheeler, V.C., White, J.K., Gutekunst, C.A., Vrbanac, V., Weaver, M., Li, X.J., Li, S.H., Yi, H., Vonsattel, J.P., Gusella, J.F. *et al.* (2000) Long glutamine tracts cause nuclear localization of a novel form of huntingtin in medium spiny striatal neurons in Hdh(Q92) and Hdh(Q111) knock-in mice. *Hum. Mol. Genet.*, **9**, 503–513.
12. Shelbourne, P.F., Killeen, N., Hevner, R.F., Johnston, H.M., Tecott, L., Lewandoski, M., Ennis, M., Ramirez, L., Li, Z., Iannicola, C. *et al.* (1999) A Huntington's disease CAG expansion at the murine *Hdh* locus is unstable and associated with behavioural abnormalities in mice. *Hum. Mol. Genet.*, **8**, 763–774.
13. Levine, M.S., Klapstein, G.J., Koppel, A., Gruen, E., Cepeda, C., Vargas, M.E., Jokel, E.S., Carpenter, E.M., Zanjani, H., Hurst, R.S. *et al.* (1999) Enhanced sensitivity to *N*-methyl-D-aspartate receptor activation in transgenic and knockin mouse models of Huntington's disease. *J. Neurosci. Res.*, **58**, 515–532.
14. Li, H., Li, S.-H., Johnston, H., Shelbourne, P.F. and Li, X.-J. (2000) Amino-terminal fragments of mutant huntingtin show selective accumulation in striatal neurons and synaptic toxicity. *Nature Genet.*, **25**, 385–389.
15. Usdin, M.T., Shelbourne, P.F., Myers, R.M. and Madison, D.V. (1999) Impaired synaptic plasticity in mice carrying the Huntington's disease mutation. *Hum. Mol. Genet.*, **8**, 839–846.
16. Stacey, A., Schnieke, A., McWhir, J., Cooper, J., Colman, A. and Melton, D.W. (1994) Use of double-replacement gene targeting to replace the murine alpha-lactalbumin gene with its human counterpart in embryonic stem cells and mice. *Mol. Cell. Biol.*, **14**, 1009–1016.
17. Ordway, J.M., Tallaksen-Greene, S., Gutekunst, C.A., Bernstein, E.M., Cearley, J.A., Wiener, H.W., Dure, L.S., Lindsey, R., Hersch, S.M., Jope, R.S. *et al.* (1997) Ectopically expressed CAG repeats cause intranuclear inclusions and a progressive late onset neurological phenotype in the mouse. *Cell*, **91**, 753–763.
18. White, J.K., Auerbach, W., Duyao, M.P., Vonsattel, J.P., Gusella, J.F., Joyner, A.L. and Macdonald, M.E. (1997) Huntingtin is required for neurogenesis and is not impaired by the Huntingtons-disease CAG expansion. *Nature Genet.*, **17**, 404–410.
19. Wexler, N.S., Young, A.B., Tanzi, R.E., Travers, H., Starosta-Rubinstein, S., Penney, J.B., Snodgrass, S.R., Shoulson, I., Gomex, F., Arroyo, M.A.R. *et al.* (1987) Homozygotes for Huntington's disease. *Nature*, **326**, 194–197.
20. Sanberg, P.R., Fibiger, H.C. and Mark, R.F. (1981) Body weight and dietary factors in Huntington's disease patients compared with matched controls. *Med. J. Aust.*, **1**, 407–409.
21. Hedreen, J.C. and Folstein, S.E. (1995) Early loss of neostriatal striosome neurons in Huntington's disease. *J. Neuropathol. Exp. Neurol.*, **54**, 105–120.
22. Ross, C.A. (1997) Intranuclear neuronal inclusions: a common pathogenic mechanism for glutamine-repeat neurodegenerative diseases? *Neuron*, **19**, 1147–1150.
23. Li, H., Li, S.H., Cheng, A.L., Mangiarini, L., Bates, G.P. and Li, X.J. (1999) Ultrastructural localization and progressive formation of neuropil aggregates in Huntington's disease transgenic mice. *Hum. Mol. Genet.*, **8**, 1227–1236.
24. Sisodia, S.S. (1998) Nuclear inclusions in glutamine repeat disorders: are they pernicious, coincidental, or beneficial? *Cell*, **95**, 1–4.
25. Mangiarini, L., Sathasivam, K., Seller, M., Cozens, B., Harper, A., Hetherington, C., Lawton, M., Trottier, Y., Lehrach, H., Davies, S.W. *et al.* (1996) Exon 1 of the HD gene with an expanded CAG repeat is sufficient to cause a progressive neurological phenotype in transgenic mice. *Cell*, **87**, 493–506.
26. Ikeda, H., Yamaguchi, M., Sugai, S., Aze, Y., Narumiya, S. and Kakizuka, A. (1996) Expanded polyglutamine in the Machado-Joseph disease protein induces cell death *in vitro* and *in vivo*. *Nature Genet.*, **13**, 196–202.
27. Ordway, J.M. and Detloff, P.J. (1996) *In vitro* synthesis and cloning of long CAG repeats. *Biotechniques*, **21**, 609–610.
28. Trottier, Y., Lutz, Y., Stevanin, G., Imbert, G., Devys, D., Cancel, G., Saudou, F., Weber, C., David, G., Tora, L. *et al.* (1995) Polyglutamine expansion as a pathological epitope in Huntington's disease and four dominant cerebellar ataxias. *Nature*, **378**, 403–406.